Microwave Zeeman Spectrum, Electric Dipole Moment and Nuclear Quadrupole Tensor of Methyl Hypochlorite and d_3-Methyl Hypochlorite

M. Suzuki * and A. Guarnieri

Abteilung Chemische Physik im Institut für Physikalische Chemie der Universität Kiel

(Z. Naturforsch. **31 a**, 1242–1258 [1976]; received June 26, 1976)

The microwave-Zeeman spectra of $CH_3O^{35}Cl$ and $CD_3O^{35}Cl$ have been investigated with magnetic fields up to 25 kG. In addition to the Zeeman parameters, the electric dipole moment and the chlorine nuclear quadrupole tensor have been determined.

Introduction

The investigation of the rotational Zeeman Spectrum of asymmetric molecules containing chlorine [1,2] is continued with this work on Methylhypochlorite and d_3-Methylhypochlorite. These molecules and other isotopic species were investigated initially some years ago by Rigden and Butcher [3] who determined the molecular structure and the barrier to internal rotation from the first torsional excited state.

As the electric dipole moment was not reported, we measured the Stark effect in both molecules and calculated the value and orientation of the total electric dipole moment.

Further the quadrupole coupling tensor was evaluated. The spectrum in the millimeterwave range is under investigation. The centrifugal distortion analysis will be the subject of a following paper.

Experimental

The methylhypochlorites, CH_3OCl and CD_3OCl, were prepared by distillation under vacuum from alkaline methyl alcohol solution saturated with chlorine gas [4]. The temperature was maintained at 0 °C during all the procedure.

As the substance decomposed in the wave guide cell at a temperature of −75 °C, it was flowed continuously through the cell during the measurements at a pressure of about 3 mTorr.

The spectrometer used was the same one reported before [1,5].

Spectrum at Zero Magnetic Field

1) Internal Rotation of the Methyl Group

Both a- and b-type transitions [3] were measured in the frequency range from 10 to 50 GHz. The b-type transitions in the ground state of $CH_3O^{35}Cl$ have been found to be slightly split into doublets due to

Table 1. A–E frequency splittings in the ground state and parameters obtained for the internal rotation of the methyl group in $CH_3O^{35}Cl$.

$J_{K_-K_+} \rightarrow J'_{K'_-K'_+}$	$\delta\nu_{A-E}$ * (obs) (MHz)	$\delta\nu_{A-E}$ (calc) (MHz)
$0_{00} \rightarrow 1_{11}$	0.170 ± 0.010	0.182
$1_{01} \rightarrow 1_{10}$	0.190 ± 0.007	0.181
$2_{02} \rightarrow 2_{11}$	0.187 ± 0.009	0.185
$4_{04} \rightarrow 4_{13}$	0.187 ± 0.006	0.199

(parameters)

$I_a = 12.0143$ amuÅ² $\quad \lambda_a = 0.7396$
$I_b = 80.2584$ $\quad \lambda_b = 0.6730$
$I_c = 89.1220$ $\quad F = 193.3$ GHz
$I = 3.11 \pm 0.05$

(barrier height)

$s = 74.5 \pm 0.5$
$V_3 = 3090 \pm 50$ cal/mole

* Average value of the A–E splittings of the nuclear quadrupole fine structure.

Table 1 A. Submatrix for $J=0$ taking into account the nuclear shielding effect.

		$M_F = \pm 3/2$	$M_F = \pm 1/2$
		$M_J=0;\ M_I=\pm 3/2$	$M_J=0;\ M_I=\pm 1/2$
$M_F = \pm 3/2$	$M_J=0$, $M_I=\pm 3/2$	$\mp\frac{3}{2} H_Z\, \mu_0\, g_I (1-\sigma)$	0
$M_F = \pm 1/2$	$M_J=0$, $M_I=\pm 1/2$	0	$\mp\frac{1}{2} H_Z\, \mu_0\, g_I (1-\sigma)$

* Present Adress: Dept of Electronic Engineering, Tokyo College of Photography. 1583, Iyama, Atsugi-Shi, *Kanagawa, 243-02*, Japan.

Reprint requests to Prof. Dr. A. Guarnieri, Institut für physikalische Chemie der Universität Kiel, Olshausenstrasse 40–60, *D-2300 Kiel*.

Table 2 a. Observed transition frequencies and frequency splittings due to the nuclear quadrupole coupling effect of the Cl atom in $CH_3O^{35}Cl$.

				$\delta\nu_{calc}$ **		
$J_{K_-K_+} \rightarrow J'_{K'_-K'_+}$	$F \rightarrow F'$	ν_{obs} *	ν_{obs}	$\delta\nu^{(1)}$	$\delta\nu^{(2)}$	$\delta\nu_{total}$
$0_{00} \rightarrow 1_{01}$ ***	$3/2 \rightarrow 1/2$	11 988.583	21.103	21.114	0.002	21.116
	$3/2 \rightarrow 5/2$	11 971.716	4.236	4.223	0.004	4.227
	$3/2 \rightarrow 3/2$	11 950.595	−16.885	−16.891	0.003	−16.888
$0_{00} \rightarrow 1_{11}$ ***	$3/2 \rightarrow 3/2$	47 739.930	5.046	5.072	0.006	5.078
	$3/2 \rightarrow 5/2$	47 733.618	−1.266	−1.268	−0.001	−1.269
	$3/2 \rightarrow 1/2$	47 728.554	−6.330	−6.340	0.011	−6.329
$1_{01} \rightarrow 1_{10}$ ***	$3/2 \rightarrow 5/2$	36 407.662	13.973	13.936	0.013	13.949
	$5/2 \rightarrow 3/2$	36 401.296	7.607	7.596	0.020	7.616
	$3/2 \rightarrow 1/2$	36 395.829	2.140	2.117	0.025	2.143
	$5/2 \rightarrow 5/2$	36 386.520	−7.169	−7.178	0.012	−7.166
	$1/2 \rightarrow 3/2$	36 384.400	−9.289	−9.295	0.021	−9.274
$1_{11} \rightarrow 2_{12}$ ***	$1/2 \rightarrow 1/2$	23 329.819	21.120	21.114	0.009	21.126
	$1/2 \rightarrow 3/2$	23 315.053	6.354	6.340	0.009	6.349
	$5/2 \rightarrow 7/2$	23 314.199	5.500	5.489	0.005	5.494
	$3/2 \rightarrow 3/2$	23 303.630	−5.069	−5.072	0.013	−5.059
	$5/2 \rightarrow 5/2$	23 299.424	−9.275	−9.285	0.012	−9.273
	$3/2 \rightarrow 5/2$	23 293.081	−15.618	−15.625	0.005	−15.620
$1_{10} \rightarrow 2_{11}$ ***	$1/2 \rightarrow 1/2$	24 582.301	21.112	21.114	−0.008	21.106
	$1/2 \rightarrow 3/2$	24 576.218	15.029	14.774	0.257	15.031
	$5/2 \rightarrow 7/2$	24 566.083	4.894	4.766	0.135	4.901
	$5/2 \rightarrow 5/2$	24 559.675	−1.514	−1.574	0.074	−1.500
	$3/2 \rightarrow 3/2$	24 549.644	−11.545	−11.819	0.262	−11.557
	$3/2 \rightarrow 5/2$	24 544.911	−16.278	−16.348	0.066	−16.282
$2_{02} \rightarrow 3_{03}$	$3/2 \rightarrow 3/2$	35 886.185	16.769	17.033	−0.251	16.782
	$5/2 \rightarrow 5/2$	35 880.241	10.825	10.874	−0.054	10.820
	$7/2 \rightarrow 9/2$	35 870.477	1.061	1.044	0.001	1.045
	$5/2 \rightarrow 7/2$	35 870.221	0.805	0.938	−0.131	0.807
	$1/2 \rightarrow 3/2$	35 865.091	−4.325	−4.152	−0.239	−4.391
	$3/2 \rightarrow 5/2$			−4.258	−0.055	−4.331
	$7/2 \rightarrow 7/2$	35 849.026	−20.390	−20.247	−0.140	−20.387
$2_{12} \rightarrow 3_{13}$	$3/2 \rightarrow 3/2$	34 973.798	16.045	16.059	−0.004	16.055
	$5/2 \rightarrow 5/2$	34 964.286	6.533	6.538	0.005	6.543
	$7/2 \rightarrow 9/2$	34 960.239	2.486	2.470	0.002	2.472
	$1/2 \rightarrow 3/2$	34 959.045	1.292	1.286	−0.004	1.282
	$5/2 \rightarrow 7/2$	34 954.927	−2.826	−2.830	−0.002	−2.832
	$3/2 \rightarrow 5/2$	34 953.732	−4.021	−4.015	−0.003	−4.018
	$7/2 \rightarrow 7/2$	34 940.150	−17.603	−17.604	0.006	−17.598
$2_{11} \rightarrow 3_{12}$	$3/2 \rightarrow 3/2$	36 845.386	9.036	9.313	−0.269	9.044
	$1/2 \rightarrow 3/2$	36 839.314	2.964	2.973	−0.004	2.969
	$7/2 \rightarrow 9/2$	36 838.274	1.924	2.069	−0.160	1.909
	$3/2 \rightarrow 5/2$	36 833.714	−2.636	−2.328	−0.300	−2.628
	$5/2 \rightarrow 7/2$	36 833.041	−3.309	−3.232	−0.083	−3.315
	$7/2 \rightarrow 7/2$	36 826.623	−9.727	−9.572	−0.144	−9.716
$2_{02} \rightarrow 2_{11}$	$5/2 \rightarrow 7/2$	37 045.300	17.097	16.944	0.154	17.098
	$5/2 \rightarrow 3/2$	37 043.604	15.401	15.132	0.289	15.421
	$5/2 \rightarrow 5/2$	37 038.905	10.702	10.603	0.093	10.697
	$3/2 \rightarrow 1/2$	37 034.557	6.359	6.340	0.023	6.363
	$3/2 \rightarrow 3/2$	37 028.508	0.305	0.000	0.288	0.288
	$7/2 \rightarrow 7/2$	37 024.145	−4.058	−4.241	0.145	−4.096
	$1/2 \rightarrow 1/2$	37 013.395	−14.808	−14.845	0.035	−14.810
	$1/2 \rightarrow 3/2$	37 007.324	−20.879	−21.185	0.300	−20.885
$3_{03} \rightarrow 3_{12}$	$7/2 \rightarrow 9/2$	38 013.333	18.218	18.074	0.125	18.199
	$5/2 \rightarrow 3/2$	38 008.752	13.637	13.571	0.072	13.643
	$7/2 \rightarrow 5/2$	38 007.084	11.969	11.866	0.120	11.986
	$7/2 \rightarrow 7/2$	38 001.694	6.579	6.433	0.142	6.575
	$5/2 \rightarrow 5/2$	37 997.085	1.970	1.930	0.041	1.971
	$9/2 \rightarrow 9/2$	37 991.888	−3.227	−3.217	−0.016	−3.233
	$3/2 \rightarrow 3/2$	37 987.695	−7.420	−7.720	0,269	−7.451
	$9/2 \rightarrow 7/2$	37 980.224	−14.891	−14.858	0.000	−14.858
	$3/2 \rightarrow 5/2$	37 975.985	−19.130	−19.361	0.238	−19.123
$4_{04} \rightarrow 4_{13}$	$9/2 \rightarrow 9/2$	39 317.468	4.831	4.865	−0.018	4.847
	$7/2 \rightarrow 7/2$	39 314.798	2.161	2.184	−0.028	2.156
	$11/2 \rightarrow 11/2$	39 309.847	−2.790	−2.780	−0.007	−2.787
	$5/2 \rightarrow 5/2$	39 307.153	−5.489	−5.461	−0.034	−5.495

* The center frequencies between the A and E lines are used for b-type transitions.

** $\delta\nu^{(1)}$ and $\delta\nu^{(2)}$ are, respectively, the first and second order effects of nuclear quadrupole coupling.

*** The nuclear quadrupole coupling constants have been determined from these transitions frequencies.

the internal rotation of the methyl group. The measured splittings are given in Table 1. Using the parameters given in the same table, the barrier height V_3 to the internal rotation of the methyl group has been determined to be 3090 ± 50 cal/mole. The result agrees with that obtained by Rigden and Butcher [3] using the splittings of the first excited torsional state.

Due to the weakness of the b-lines, the torsional fine structure below 200 kHz could not be resolved in Stark and Zeeman measurements, as the pressure in the cell has to be raised. So we were forced to use the center frequency of the doublets for the analysis given later.

This introduced only a minor error as the barrier to internal rotation is high.

The internal rotation splittings in $CD_3O^{35}Cl$ have not been observed due to the higher value of the reduced barrier height s.

2) Nuclear Quadrupole Coupling Constants

As indicated by the waved lines in the level scheme of Fig. 1 some levels show near degeneracies. An anomalous contribution respect to a first order treatment was observed in the hfs-splittings of those transitions connected to one of the two levels 2_{11} or 3_{03}. The analysis of the $0_{00} \rightarrow 1_{01}$, $0_{00} \rightarrow 1_{11}$, $1_{01} \rightarrow 1_{10}$ and $1_{11} \rightarrow 2_{12}$ transitions of $CH_3O^{35}Cl$, listed in Table 2 a, resulted in χ_{aa}^{Cl} and χ_{bb}^{Cl} values given in Table 4.

These χ^{Cl}-values reproduce the observed hfs-splittings $\delta\nu_{obs}$ by first order perturbation theory $\delta\nu^{(1)}$ within experimental accuracy, but failed to reproduce hfs-splittings $\delta\nu_{obs}$ of the $1_{10} \rightarrow 2_{11}$ transition. The $(\delta\nu_{obs} - \delta\nu^{(1)})$ values were used to calculate the out off diagonal element χ_{ab}^{Cl} by second order perturbation theory according to Bragg [6]. The χ_{ab}^{Cl} value given in Table 4 accounts for all $(\delta\nu_{obs} - \delta\nu^{(1)})$ of Table 2 b.

For $CD_3O^{35}Cl$ the χ_{aa}^{Cl} and χ_{bb}^{Cl} values were determined from the same set of transitions. In this case both levels of the $1_{10} \rightarrow 2_{11}$ transition are influenced by near degeneracies, as indicated in Figure 1. The used frequencies may be found in Table 2 c. The χ^{Cl}-values are listed in Table 4. The rigid rotor rotational constants of Table 4 for both isotopic species have been calculated from the hfs-unperturbed transition frequencies given in Table 3. The rotational constants agree with those reported by Rigden and Butcher [3].

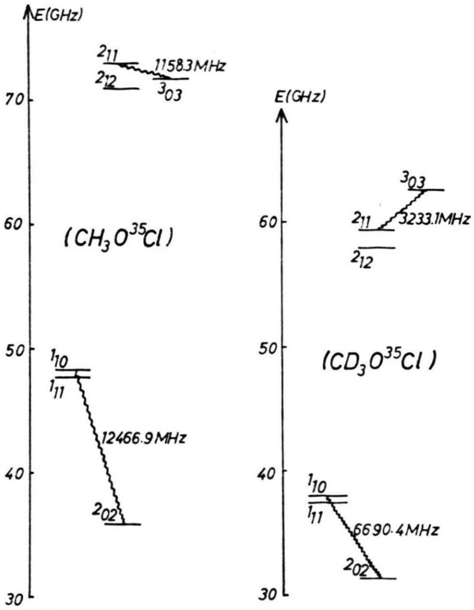

Fig. 1. Near degeneracy in methylhypochlorite. The energy levels connected with the waved line have a second order perturbation contribution due to the χ_{ab}^{Cl} term.

Table 2 b. Second order contribution in the $1_{10} \rightarrow 2_{11}$ line in $CH_3O^{35}Cl$.

$F \rightarrow F'$	$\delta\nu_{obs}^{(2)}$ * kHz	$\delta\nu_{calc}^{(2)}$ ** kHz
$1/2 \rightarrow 1/2$	0	0
$1/2 \rightarrow 3/2$	257	267
$5/2 \rightarrow 7/2$	130	143
$5/2 \rightarrow 5/2$	62	76
$3/2 \rightarrow 3/2$	276	267
$3/2 \rightarrow 5/2$	72	76

* $\delta\nu_{obs}^{(2)}\ (F \rightarrow F') = \nu_{obs}(F \rightarrow F') - \{\delta\nu^{(1)}(F \rightarrow F') + \nu_{obs}^{0}\}$ where $\nu_{obs}^{0} = \nu_{obs}(1/2 \rightarrow 1/2) - \delta\nu^{(1)}(1/2 \rightarrow 1/2)$

** $\delta\nu_{calc}^{(2)} = |\langle 2_{11}, 3/2, F, M_F = F \,|\, \mathcal{H}_Q \,|\, 3_{03}, 3/2, F, M_F = F \rangle|^2 / (E_{2_{11}} - E_{3_{03}})$

The determination of the off-diagonal element of the nuclear quadrupole coupling tensor allows the transformation of the coupling tensor to its principal axis system. The result (set I) is listed in Table 5 in comparison with a set II obtained from the isotopic substitution effect. The agreement between the two sets is quite good.

Further the transformation angle, $\Theta_{za} = 25.6 \pm 0.3^0$, between the principal inertial axis system and the principal axis system of the coupling tensor practically coincides with the value of 24.8 ± 1.4^0 (see [3]) of the angle between the Cl – O bond and the a-principal axis. Since the χ_{zz}^{Cl} value in this paper is almost

Table 2 c. Observed transition frequencies and frequency splittings due to the nuclear quadrupole coupling effect of the Cl atom in $CD_3O^{35}Cl$.

$J_{K_-K_+} \to J'_{K'_-K'_+}$	$F \to F'$	ν_{obs}	$\delta\nu_{obs}$	$\delta\nu_{calc}$: $\delta\nu^{(1)}$	$\delta\nu^{(2)}$	$\delta\nu_{total}$
$0_{00} \to 1_{01}$ *	$3/2 \to 1/2$	10 460.234	20.006	20.012	0.000	20.012
	$3/2 \to 5/2$	10 444.236	4.008	4.002	0.004	4.006
	$3/2 \to 3/2$	10 424.225	−16.003	−16.009	0.001	−16.008
$0_{00} \to 1_{11}$ *	$3/2 \to 3/2$	37 518.112	4.225	4.214	0.010	4.224
	$3/2 \to 5/2$	37 512.849	−1.038	−1.054	0.000	−1.054
	$3/2 \to 1/2$	37 508.619	−5.268	−5.268	0.015	−5.253
$1_{01} \to 1_{10}$ *	$3/2 \to 3/2$	27 591.781	27.840	27.804	0.041	27.845
	$3/2 \to 5/2$	27 577.041	13.100	13.061	0.026	13.087
	$5/2 \to 3/2$	27 571.758	7.817	7.793	0.039	7.832
	$3/2 \to 1/2$	27 565.254	1.313	1.266	0.051	1.317
	$5/2 \to 5/2$	27 557.022	−6.916	−6.951	0.023	−6.928
	$1/2 \to 3/2$	27 555.776	−8.165	−8.217	0.043	−8.174
	$1/2 \to 1/2$	27 529.230	−34.711	−34.755	0.052	−34.703
$1_{11} \to 2_{12}$ *	$1/2 \to 1/2$	20 410.166	20.022	20.012	0.006	20.018
	$3/2 \to 1/2$	20 400.675	10.531	10.530	0.012	10.542
	$1/2 \to 3/2$ $5/2 \to 7/2$	20 395.417	5.273	5.268 5.266	0.008 0.005	5.271 5.271
	$5/2 \to 3/2$	20 391.193	1.049	1.054	0.023	1.077
	$3/2 \to 3/2$	20 385.932	−4.212	−4.214	0.013	−4.201
	$5/2 \to 5/2$	20 380.670	−9.474	−9.478	0.012	−9.466
	$3/2 \to 5/2$	20 375.412	−14.732	−14.746	0.003	−14.743
$1_{10} \to 2_{11}$ *	$1/2 \to 1/2$	21 390.622	19.987	20.012	−0.030	19.982
	$1/2 \to 3/2$	21 385.254	14.619	14.744	−0.133	14.611
	$5/2 \to 7/2$	21 375.019	4.384	4.454	−0.073	4.381
	$5/2 \to 3/2$	21 373.467	2.832	2.949	−0.108	2.841
	$5/2 \to 5/2$	21 369.774	−0.861	−0.814	−0.041	−0.855
	$3/2 \to 1/2$	21 364.076	−6.559	−6.527	−0.021	−6.548
	$3/2 \to 3/2$	21 358.716	−11.919	−11.795	−0.123	−11.918
	$3/2 \to 5/2$	21 355.030	−15.605	−15.558	−0.057	−16.615
$4_{04} \to 4_{13}$	$9/2 \to 9/2$	29 856.549	5.107	5.119	−0.014	5.105
	$7/2 \to 7/2$	29 853.711	2.269	2.298	−0.046	2.252
	$11/2 \to 11/2$	29 848.488	−2.954	−2.925	−0.006	−2.931
	$5/2 \to 5/2$	29 845.661	−5.781	−5.746	−0.039	−5.785
$5_{05} \to 5_{14}$	$11/2 \to 11/2$	31 183.472	4.433	4.429	−0.010	4.419
	$9/2 \to 9/2$	31 181.432	2.393	2.399	0.004	2.403
	$13/2 \to 13/2$	31 176.262	−2.777	−2.768	−0.004	−2.772
	$7/2 \to 7/2$	31 174.233	−4.806	−4.798	−0.007	−4.805

* The nuclear quadrupole coupling constants have been determined from these transition frequencies.

equal to that of $HO^{35}Cl$ [7], we may conclude that the bond character is almost the same in both molecules.

Zeeman Spectrum

1) Zeeman Parameters

The Zeeman splitting of the $0_{00} \to 1_{11}$, $0_{00} \to 1_{01}$, $1_{01} \to 1_{10}$, $1_{10} \to 2_{11}$ and $1_{11} \to 2_{12}$ transitions were measured at magnetic fields up to 25 kG with perpendicular and parallel field. The method described in Ref. [1] was modified to account for the nuclear shielding effect, when determining the Zeeman parameters.

The effective Hamiltonian for the shielded nuclear Zeeman effect has been given by Hüttner and Flygare [8] as follows:

$$\mathcal{H}^{(\mathrm{I})}_{\mathrm{mag}} = -\mu_0\, g_I (1-\sigma)\, H_Z I_Z + \mu_0\, g_I\, H_Z I_Z \sum_g \sigma_{gg} (\Phi^2_{gZ} - \tfrac{1}{3}) \qquad (1)$$

where μ_0 is the nuclear magneton, g_I the nuclear g-factor of the Cl-atom, H_Z the applied field, σ_{gg} are diagonal elements of the nuclear shielding tensor with respect to the principal inertial axis system and σ is the nuclear shielding factor defined by

$$\sigma = \tfrac{1}{3} (\sigma_{aa} + \sigma_{bb} + \sigma_{cc}) \,. \qquad (2)$$

Using $|J\,\tau\, I\, M_J\, M_I\rangle$ as basic wave functions the first order energy expression has been obtained by the method given before [1] modifying the equation

$$E^{(\mathrm{I})}_{\mathrm{mag}} = -\mu_0\, g_I\, M_I\, H_Z \quad \text{of Ref. [1]} \qquad (3)$$

Table 2 A. Part of the submatrix for $J=1$ taking into account the nuclear shielding effect.

		$M_F=\pm 5/2$	$M_F=\pm 3/2$	
		$M_J=\pm 1;\ M_I=\pm 3/2$	$M_J=\pm 1;\ M_I=\pm 1/2$	$M_J=0;\ M_I=\pm 3/2$
$M_F=\pm 5/2$	$M_J=\pm 1$ $M_I=\pm 3/2$	$\mp\frac{3}{2}H_Z\mu_0 g_I(1-\sigma)$ $\pm\frac{1}{10}H_Z\mu_0 g_I\sum_g(3\sigma_{gg}-3\sigma)\langle J_g^2\rangle_{1\tau}$ $\mp\frac{1}{2}H_Z\mu_0\sum_g g_{gg}\langle J_g^2\rangle_{1\tau}$ $-\frac{1}{30}H_z^2\sum_g(3\chi_{gg}-3\chi)\langle J_g^2\rangle_{1\tau}$ $+\frac{1}{20}\sum_g\chi_{gg}^{\mathrm{Cl}}\langle J_g^2\rangle_{1\tau}$	0	0
$M_F=\pm 3/2$	$M_J=\pm 1$ $M_I=\pm 1/2$	0	$\mp\frac{1}{2}H_Z\mu_0 g_I(1-\sigma)$ $\pm\frac{1}{30}H_Z\mu_0 g_I\sum_g(3\sigma_{gg}-3\sigma)\langle J_g^2\rangle_{1\tau}$ $\mp\frac{1}{2}H_Z\mu_0\sum_g g_{gg}\langle J_g^2\rangle_{1\tau}$ $-\frac{1}{30}H_z^2\sum_g(3\chi_{gg}-3\chi)\langle J_g^2\rangle_{1\tau}$ $-\frac{1}{20}\sum_g\chi_{gg}^{\mathrm{Cl}}\langle J_g^2\rangle_{1\tau}$	$\frac{\sqrt{6}}{20}\sum_g\chi_{gg}^{\mathrm{Cl}}\langle J_g^2\rangle_{1\tau}$
	$M_J=0$ $M_I=\pm 3/2$	0	$\frac{\sqrt{6}}{20}\sum_g\chi_{gg}^{\mathrm{Cl}}\langle J_g^2\rangle_{1\tau}$	$\mp\frac{3}{2}H_Z\mu_0 g_I(1-\sigma)$ $\mp\frac{1}{5}H_Z\mu_0 g_I$ $\cdot\sum_g(3\sigma_{gg}-3\sigma)\langle J_g^2\rangle_{1\tau}$ $-\frac{1}{15}H_z^2$ $\cdot\sum_g(3\chi_{gg}-3\chi)\langle J_g^2\rangle_{1\tau}$ $-\frac{1}{10}\sum_g\chi_{gg}^{\mathrm{Cl}}\langle J_g^2\rangle_{1\tau}$

to

$$E_{\mathrm{mag}}^{(\mathrm{I})}=-\mu_0 g_I(1-\sigma)M_I H_Z+\mu_0 g_I\frac{2M_I\{3M_J{}^2-J(J+1)\}}{3J(J+1)(2J-1)(2J+3)}\cdot H_Z\sum_g(3\sigma_{gg}-3\sigma)\langle J_\tau{}^2\rangle \tag{4}$$

where $\langle J_\tau{}^2\rangle$ is the expectation value of the squared angular momentum for the state J_τ. The matrix elements used in this analysis are given in Appendix I.

Following the procedure of Ref. [1], the functions

$$\Delta_i(g_I,g_{aa},g_{bb},g_{cc},\sigma_\alpha,\sigma_\beta)\quad\text{and}\quad S_i(\alpha,\beta)$$

listed in Table 6 have been used. σ_α and σ_β are the nuclear shielding anisotropies

$$\sigma_\alpha=2\sigma_{aa}-\sigma_{bb}-\sigma_{cc}\,;\qquad\sigma_\beta=2\sigma_{bb}-\sigma_{cc}-\sigma_{aa}\,.$$

α and β are the magnetic susceptibility anisotropies

$$\alpha=2\chi_{aa}-\chi_{bb}-\chi_{cc}\,;\qquad\beta=2\chi_{bb}-\chi_{cc}-\chi_{aa}\,.$$

The values of D_ν^- and D_ν^+ [1] calculated from the observed Zeeman satellites are given in Table 7 a and 7 b.

Table 3. Unperturbed transition frequencies of $CH_3O^{35}Cl$ and $CD_3O^{35}Cl$ in MHz.

$J_{K_-K_+}\rightarrow J'_{K'_-K'_+}$	ν^0_{obs} *	$\nu^0_{\mathrm{obs}}-\nu^0_{\mathrm{calc}}$
$CH_3O^{35}Cl$		
$0_{00}\rightarrow 1_{01}$ **	11 967.480 ± 0.008	0.009
$0_{00}\rightarrow 1_{11}$ **	47 734.884 ± 0.008	−0.012
$1_{01}\rightarrow 1_{10}$ **	36 393.689 ± 0.006	0.012
$1_{11}\rightarrow 2_{12}$ **	23 308.699 ± 0.006	0.007
$1_{10}\rightarrow 2_{11}$ **	24 561.189 ± 0.006	−0.005
$2_{02}\rightarrow 3_{03}$	35 869.416 ± 0.010	−0.399
$2_{12}\rightarrow 3_{13}$	34 957.753 ± 0.008	−0.222
$2_{11}\rightarrow 3_{12}$	36 836.350 ± 0.010	−0.312
$2_{02}\rightarrow 2_{11}$	37 028.203 ± 0.010	0.123
$3_{03}\rightarrow 3_{12}$	37 995.115 ± 0.025	0.188
$4_{04}\rightarrow 4_{13}$	39 312.637 ± 0.012	0.276
$CD_3O^{35}Cl$		
$0_{00}\rightarrow 1_{01}$ **	10 440.228 ± 0.005	0.030
$0_{00}\rightarrow 1_{11}$ **	37 513.887 ± 0.005	−0.003
$1_{01}\rightarrow 1_{10}$ **	27 563.941 ± 0.003	0.002
$1_{11}\rightarrow 2_{12}$ **	20 390.144 ± 0.003	0.006
$1_{10}\rightarrow 2_{11}$ **	21 370.635 ± 0.003	−0.007
$4_{04}\rightarrow 4_{13}$	29 851.442 ± 0.016	0.027
$5_{05}\rightarrow 5_{14}$	31 179.039 ± 0.010	−0.134

* The center frequencies between the A and E lines are given for the b-type transitions in $CH_3O^{35}Cl$.
** The rotational constants have been calculated from these transition frequencies.

Table 3 A. Part of the submatrix for $J=2$ taking into account the nuclear shielding effect.

		$M_F=\pm 7/2$	$M_F=\pm 5/2$	
		$M_J=\pm 2;\ M_I=\pm 3/2$	$M_J=\pm 2;\ M_I=\pm 1/2$	$M_J=\pm 1;\ M_I=\pm 3/2$
$M_F=\pm 7/2$	$M_J=\pm 2$ $M_I=\pm 3/2$	$\mp \frac{3}{2} H_Z \mu_0 g_I (1-\sigma)$ $\pm \frac{1}{21} H_Z \mu_0 g_I \sum_g (3\sigma_{gg}-3\sigma) \langle J_g^2 \rangle_{2\tau}$ $\mp \frac{1}{3} H_Z \mu_0 \sum_g g_{gg} \langle J_g^2 \rangle_{2\tau}$ $-\frac{1}{63} H_Z^2 \sum_g (3\chi_{gg}-3\chi) \langle J_g^2 \rangle_{2\tau}$ $+\frac{1}{42} \sum_g \chi_{gg}^{Cl} \langle J_g^2 \rangle_{2\tau}$	0	0
$M_F=\pm 5/2$	$M_J=\pm 2$ $M_I=\pm 1/2$	0	$\mp \frac{1}{2} H_Z \mu_0 g_I (1-\sigma)$ $\pm \frac{1}{63} H_Z \mu_0 g_I \sum_g (3\sigma_{gg}-3\sigma) \langle J_g^2 \rangle_{2\tau}$ $\mp \frac{1}{3} H_Z \mu_0 \sum_g g_{gg} \langle J_g^2 \rangle_{2\tau}$ $-\frac{1}{63} H_Z^2 \sum_g (3\chi_{gg}-3\chi) \langle J_g^2 \rangle_{2\tau}$ $-\frac{1}{42} \sum_g \chi_{gg}^{Cl} \langle J_g^2 \rangle_{2\tau}$	$\frac{\sqrt{3}}{42} \sum_g \chi_{gg}^{Cl} \langle J_g^2 \rangle_{2\tau}$
	$M_J=\pm 1$ $M_I=\pm 3/2$	0	$\frac{\sqrt{3}}{42} \sum_g \chi_{gg}^{Cl} \langle J_g^2 \rangle_{2\tau}$	$\mp \frac{3}{2} H_Z \mu_0 g_I (1-\sigma)$ $\mp \frac{1}{42} H_Z \mu_0 g_I$ $\sum_g (3\sigma_{gg}-3\sigma) \langle J_g^2 \rangle_{2\tau}$ $\mp \frac{1}{6} H_Z \mu_0 \sum_g g_{gg} \langle J_g^2 \rangle_{2\tau}$ $+\frac{1}{126} H_Z^2$ $\sum_g (3\chi_{gg}-3\chi) \langle J_g^2 \rangle_{2\tau}$ $-\frac{1}{84} \sum_g \chi_{gg}^{Cl} \langle J_g^2 \rangle_{2\tau}$

Table 4. Rotational constants and nuclear quadrupole coupling constants for $CH_3O^{35}Cl$ and $CD_3O^{35}Cl$ in MHz.

	$CH_3O^{35}Cl$	$CD_3O^{35}Cl$
A	42 064.286 ± 0.011	32 538.914 ± 0.016
B	6 296.861 ± 0.006	5 465.222 ± 0.008
C	5 670.610 ± 0.005	4 974.976 ± 0.008
χ_{aa}^{Cl}	−84.456 ± 0.026	−80.045 ± 0.011
χ_{bb}^{Cl}	25.361 ± 0.022	21.072 ± 0.011
χ_{cc}^{Cl} *	59.095	58.973
χ_{ab}^{Cl}	68.2 ± 1.3	70 ± 3

* χ_{cc}^{Cl} is calculated by the relation $\chi_{aa}^{Cl}+\chi_{bb}^{Cl}+\chi_{cc}^{Cl}=0$.

For the $1_{01} \rightarrow 1_{10}$ transition the D_ν^- and D_ν^+ are:

$$D_\nu^- = \nu\,(F=5/2 \rightarrow 5/2,\, M_F=-5/2 \rightarrow -5/2;\, H_Z) - \nu\,(F=5/2 \rightarrow 5/2,\, M_F=5/2 \rightarrow 5/2;\, H_Z) = \frac{\mu_0 H_Z}{h} \Delta_3(g_I, g_{aa}, g_{bb}, g_{cc}, \sigma_\alpha, \sigma_\beta)\,, \tag{5}$$

$$D_\nu^+ = \{\nu\,(F=5/2 \rightarrow 5/2,\, M_F=-5/2 \rightarrow -5/2;\, H_Z) + \nu\,(F=5/2 \rightarrow 5/2,\, M_F=5/2 \rightarrow 5/2;\, H_Z)\} - 2\,\nu\,(F=5/2 \rightarrow 5/2;\, H_Z=0) = \frac{H_Z^2}{h} S_3(\alpha,\beta)\,. \tag{6}$$

Table 5. Nuclear quadrupole coupling constants in the bond axis system (MHz).

	$CH_3O^{35}Cl$ I *	$CH_3O^{35}Cl$ II **	$HO^{35}Cl$ ***
χ_{zz}^{Cl}	−117.1 ± 2.0	−119.5 ± 2.6	−121.86 ± 0.28
χ_{xx}^{Cl}	58.0 ± 2.0	60.5 ± 2.6	59.56 ± 0.25
χ_{yy}^{Cl}	59.1	59.1	62.30
Θ_{za}	25.6 ± 0.3°	26.2 ± 0.7	—
$\eta = \frac{\chi_{xx}^{Cl}-\chi_{yy}^{Cl}}{\chi_{zz}^{Cl}}$	0.009 ± 0.017	−0.012 ± 0.023	0.022 ± 0.004

* Calculated from the χ_{ab}^{Cl} value.
** Calculated from the isotopic substitution effect.
*** Reference 7.

Table 6. List of the functions $\Delta_i(g_I, g_{aa}, g_{bb}, g_{cc}, \sigma_a, \sigma_\beta)$ and $S_i(\alpha, \beta)$.

i	$J_{K_-K_+} \to J'_{K'_-K'_+}$	F	$\lvert M_F \rvert \to \lvert M_F \rvert'$	$\Delta_i(g_I, g_{aa}, g_{bb}, g_{cc}, \sigma_a, \sigma_\beta)$	$S_i(\alpha, \beta)$
(‖-field)					
1.	$0_{00} \to 1_{11}$	3/2	$3/2 \to 3/2$	$-g_I(1-\sigma)+\frac{1}{2}(g_{aa}+g_{cc})-\frac{1}{6}g_I\sigma_\beta$	$-\frac{1}{30}\beta$
2.	$0_{00} \to 1_{01}$	3/2	$3/2 \to 3/2$	$-g_I(1-\sigma)+\frac{1}{2}(g_{bb}+g_{cc})-\frac{1}{6}g_I\sigma_a$	$-\frac{1}{30}\alpha$
3.	$1_{01} \to 1_{10}$	5/2	$5/2 \to 5/2$	$g_{aa}-g_{cc}-\frac{1}{5}g_I(2\sigma_a+\sigma_\beta)$	$-\frac{1}{15}(2\alpha+\beta)$
4.	$1_{10} \to 2_{11}$	5/2	$5/2 \to 5/2$	$-g_I(1-\sigma)-\frac{1}{2}g_{aa}+g_{bb}+\frac{1}{2}g_{cc}+\frac{1}{210}g_I(42\sigma_a+47\sigma_\beta)$	$\frac{1}{210}(14\alpha+9\beta)$
5.	$1_{11} \to 2_{12}$	5/2	$5/2 \to 5/2$	$-g_I(1-\sigma)-\frac{1}{2}g_{aa}+\frac{1}{2}g_{bb}+g_{cc}-\frac{1}{210}g_I(5\sigma_a+47\sigma_\beta)$	$\frac{1}{210}(5\alpha-9\beta)$
(⊥-field)					
6.	$0_{00} \to 1_{11}$	3/2	$3/2 \to 5/2$	$g_{aa}+g_{cc}+\frac{1}{5}g_I\sigma_\beta$	$\frac{1}{15}\beta$
7.	$0_{00} \to 1_{01}$	3/2	$3/2 \to 5/2$	$g_{bb}+g_{cc}+\frac{1}{5}g_I\sigma_a$	$\frac{1}{15}\alpha$
8.	$0_{00} \to 1_{01}$	3/2	$1/2 \to 3/2$	$g_I(1-\sigma)+\frac{1}{2}(g_{bb}+g_{cc})-\frac{1}{6}g_I\sigma_a$	$-\frac{1}{30}\alpha$
9.	$1_{10} \to 2_{11}$	5/2	$5/2 \to 7/2$	$\frac{1}{3}(-g_{aa}+5g_{bb}+2g_{cc})+\frac{1}{35}g_I(7\sigma_a-3\sigma_\beta)$	$\frac{1}{105}(7\alpha-3\beta)$
10.	$1_{11} \to 2_{12}$	5/2	$5/2 \to 7/2$	$\frac{1}{3}(-g_{aa}+2g_{bb}+5g_{cc})+\frac{1}{35}g_I(10\sigma_a+3\sigma_\beta)$	$\frac{1}{105}(10\alpha+3\beta)$

The assignment of Zeeman satellites has been done measuring the relative intensities and the frequency displacements at the different magnetic fields.

The values of the functions Δ_i and S_i listed in Table 8 have been obtained by using the relations given as footnote in the same Table.

The sign of the molecular g-factors is based on a positive value of the g_I-factor of chlorine atom [9].

The values for both molecular species are listed in Table 9. For comparison the molecular g-factors have been calculated including the nuclear shielding anisotropies.

However, as shown in Table 9, these molecular g-factors do not differ significantly from those obtained without inclusion of the nuclear shielding anisotropies. These anisotropies are rather undetermined, as their standard errors equal their values. For these reasons we omit them from the discussion.

The values of the magnetic susceptibility anisotropies α and β were determined with the help of Fig. 2, where a plot of α over β for each $S_i(\alpha, \beta)$ function is reported. The possible values of α and β are taken from the common region limited by the lines which define the error limit of the plotted curves. The determined values are listed in Table 9.

2) Description of the Zeeman Pattern

As neither (F, M_F) nor (M_J, M_I) are good quantum numbers at intermediate fields, the energy levels

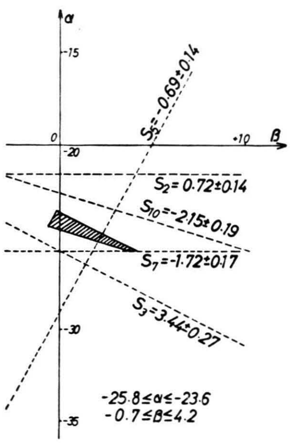

Fig. 2. Plot of α over β for each $S_i(\alpha, \beta)$ function in $CH_3O^{35}Cl$. a) α, β are magnetic susceptibility anisotropies. b) Units are in 10^{-6} erg/G^2 mole. c) The possible values of α and β are determined by the shaded area wich defines the common region limited by the lines designating the error limits of the plotted curves.

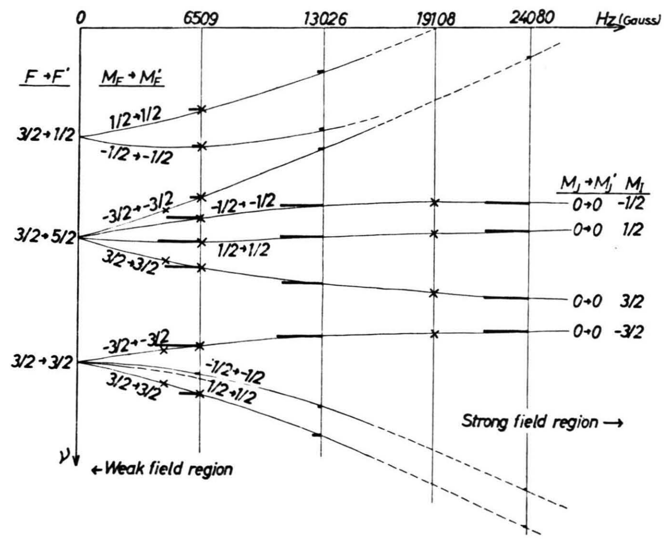

Fig. 3. Zeeman splittings of the $J=0_{00} \to J=1_{11}$ transition at parallel field in CH_3OCl. a) The relative intensities are given by the thick lines. b) Frequency measurements were done at the cross points.

Table 7 a. Values of D_ν^- and D_ν^+ in $CH_3O^{35}Cl$.

$J_{K_-K_+} \rightarrow J'_{K'_-K'_+}$	H (Gauss)	$F \rightarrow F'$	$M_F \rightarrow M_{F'}$	ν_{obs} (MHz)	D_ν^- (MHz) obs.	D_ν^- (MHz) calc.	D_ν^+ (kHz) obs.	D_ν^+ (kHz) calc.
(‖-field)								
$0_{00} \rightarrow 1_{11}$	0.0	$3/2 \rightarrow 3/2$		47 739.946	0.0	0.000		
		$3/2 \rightarrow 5/2$		47 733.618				
		$3/2 \rightarrow 3/2$	$3/2 \rightarrow 3/2$	47 740.982				
			$-3/2 \rightarrow -3/2$	47 739.293				
	4 594.6				−2.093	−2.089	—	—
		$3/2 \rightarrow 5/2$	$3/2 \rightarrow 3/2$	47 734.728				
			$-3/2 \rightarrow -3/2$	47 732.232				
		$3/2 \rightarrow 3/2$	$3/2 \rightarrow 3/2$	47 741.496				
			$-3/2 \rightarrow -3/2$	47 739.094				
	6 508.8				−2.949	−2.959		
		$3/2 \rightarrow 5/2$	$3/2 \rightarrow 3/2$	47 735.083				
			$-3/2 \rightarrow -3/2$	47 731.586				
$0_{00} \rightarrow 1_{01}$	0.0	$3/2 \rightarrow 5/2$		11 971.716	0.0	0.000	0	0
		$3/2 \rightarrow 3/2$		11 950.595				
		$3/2 \rightarrow 5/2$	$3/2 \rightarrow 3/2$	11 975.507				
			$-3/2 \rightarrow -3/2$	11 968.679				
	13 026.4				−5.774	−5.750	0	35
		$3/2 \rightarrow 3/2$	$3/2 \rightarrow 3/2$	11 952.578				
			$-3/2 \rightarrow -3/2$	11 947.858				
		$3/2 \rightarrow 5/2$	$3/2 \rightarrow 3/2$	11 977.480				
			$-3/2 \rightarrow -3/2$	11 967.558				
	19 111.9				−8.435	−8.436	64	75
		$3/2 \rightarrow 3/2$	$3/2 \rightarrow 3/2$	11 953.329				
			$-3/2 \rightarrow -3/2$	11 946.382				
		$3/2 \rightarrow 5/2$	$3/2 \rightarrow 3/2$	11 979.163				
			$-3/2 \rightarrow -3/2$	11 966.776				
	24 077.1				−10.641	−10.629	105	119
		$3/2 \rightarrow 3/2$	$3/2 \rightarrow 3/2$	11 953.894				
			$-3/2 \rightarrow -3/2$	11 944.999				
$1_{01} \rightarrow 1_{10}$	0.0	$5/2 \rightarrow 5/2$		36 386.520	0.0	0.000	0	0
	24 075.8	$5/2 \rightarrow 5/2$	$5/2 \rightarrow 5/2$	36 386.970	−0.405	−0.408	495	460
			$-5/2 \rightarrow -5/2$	36 386.565				
	25 567.5	$5/2 \rightarrow 5/2$	$5/2 \rightarrow 5/2$	36 387.026	−0.444	−0.433	568	519
			$-5/2 \rightarrow -5/2$	36 386.582				
$1_{10} \rightarrow 2_{11}$		$5/2 \rightarrow 7/2$		24 566.083				
	0.0				0.0	0.000	0	0
		$5/2 \rightarrow 5/2$		24 559.675				
		$5/2 \rightarrow 7/2$	$5/2 \rightarrow 5/2$	24 567.953				
			$-5/2 \rightarrow -5/2$	24 565.094				
	7 805.6				−3.322	−3.342	−6	−24
		$5/2 \rightarrow 5/2$	$5/2 \rightarrow 5/2$	24 561.121				
			$-5/2 \rightarrow -5/2$	24 557.336				
		$5/2 \rightarrow 7/2$	$5/2 \rightarrow 5/2$	24 569.193				
			$-5/2 \rightarrow -5/2$	24 564.758				
	11 739.2				−5.035	−5.026	−37	−55
		$5/2 \rightarrow 5/2$	$5/2 \rightarrow 5/2$	24 561.563				
			$-5/2 \rightarrow -5/2$	24 555.928				
		$5/2 \rightarrow 7/2$	$5/2 \rightarrow 5/2$	24 571.820				
			$-5/2 \rightarrow -5/2$	24 564.405				
	19 106.2				−8.166	−8.181	−125	−144
		$5/2 \rightarrow 5/2$	$5/2 \rightarrow 5/2$	24 561.979				
			$-5/2 \rightarrow -5/2$	24 553.063				
		$5/2 \rightarrow 7/2$	$5/2 \rightarrow 5/2$	24 574.314				
			$-5/2 \rightarrow -5/2$	24 564.203				

$J_{K_{-}K_{+}} \to J'_{K'_{-}K'_{+}}$	H (Gauss)	$F \to F'$	$M_F \to M_F'$	ν_{obs} (MHz)	D_ν^- (MHz) obs	D_ν^- (MHz) calc.	D_ν^+ (kHz) obs.	D_ν^+ (kHz) calc.
	25 565.1				−10.951	−10.946	−222	−257
		5/2 → 5/2	5/2 → 5/2	24 562.173				
			−5/2 → −5/2	24 550.383				
$1_{11} \to 2_{12}$		5/2 → 7/2		23 314.199				
	0.0				0.0	0.000	0	0
		5/2 → 5/2		23 299.424				
		5/2 → 7/2	5/2 → 5/2	23 316.162				
			−5/2 → −5/2	23 312.277				
	9 136.5				−3.956	−3.956	−20	−14
		5/2 → 5/2	5/2 → 5/2	23 301.397				
			−5/2 → −5/2	23 296.871				
		5/2 → 7/2	5/2 → 5/2	23 317.510				
			−5/2 → −5/2	23 312.179				
	14 301.2				−6.203	−6.191	−36	−34
		5/2 → 5/2	5/2 → 5/2	23 302.277				
			−5/2 → −5/2	23 295.208				
		5/2 → 7/2	5/2 → 5/2	23 318.881				
			−5/2 → −5/2	23 311.742				
	19 118.3				−8.272	−8.277	−66	−60
		5/2 → 5/2	5/2 → 5/2	23 302.948				
			−5/2 → −5/2	23 293.543				
		5/2 → 7/2	5/2 → 5/2	23 320.429				
			−5/2 → −5/2	23 311.373				
	24 083.5				−10.438	−10.427	−100	−97
		5/2 → 7/2	5/2 → 5/2	23 303.532				
			−5/2 → −5/2	23 291.712				
(⊥-field)								
$0_{00} \to 1_{11}$	0.0	3/2 → 5/2		47 733.618	0.0	0.000	–	–
	21 975.8	3/2 → 5/2	3/2 → 5/2	47 734.423	−1.644	−1.632	–	–
			−3/2 → −5/2	47 732.779				
$0_{00} \to 1_{01}$	0.0	3/2 → 5/2		11 971.716	0.0	0.000	0	0
	9 796.3	3/2 → 5/2	3/2 → 5/2	11 971.926	−0.448	−0.468	−28	−40
			−3/2 → −5/2	11 971.478				
	14 691.1	3/2 → 5/2	3/2 → 5/2	11 972.018	−0.697	−0.703	−93	−89
			−3/2 → −5/2	11 971.321				
	21 958.0	3/2 → 5/2	3/2 → 5/2	11 972.131	−1.038	−1.049	−208	−199
			−3/2 → −5/2	11 971.093				
		3/2 → 5/2		11 971.716				
	0.0				0.0	0.000	–	–
		3/2 → 3/2		11 950.595				
		3/2 → 5/2	−1/2 → −3/2	11 973.452				
			1/2 → 3/2	11 970.418				
	9 796.3				3.871	3.857		
		3/2 → 3/2	−1/2 → −3/2	11 952.758				
			1/2 → 3/2	11 948.050				
		3/2 → 5/2	−1/2 → −3/2	11 974.484				
			1/2 → 3/2	11 969.900				
	14 702.1				5.787	5.787	–	–
		3/2 → 3/2	−1/2 → −3/2	11 953.647				
			1/2 → 3/2	11 946.656				
$1_{11} \to 2_{12}$	0.0	5/2 → 7/2		23 314.199	0.0	0.000	0	0
	14 291.5	5/2 → 7/2	5/2 → 7/2	23 314.468	−0.640	−0.648	−102	−118
			−5/2 → −7/2	23 313.828				
	23 992.0	5/2 → 7/2	5/2 → 7/2	23 314.591	−1.093	−1.088	−309	−332
			−5/2 → −7/2	23 313.498				

Table 7 b. Values of D_ν^- and D_ν^+ in $CD_3O^{35}Cl$.

$J_{K_-K_+} \to J'_{K'_-K'_+}$	H (Gauss)	$F \to F'$	$M_F \to M_F'$	ν_{obs} (MHz)	D_ν^- (MHz) obs.	D_ν^- (MHz) calc. *	D_ν^+ (kHz) obs.	D_ν^+ (kHz) calc. *
(‖-field)								
$0_{00} \to 1_{11}$	0.0	3/2 → 3/2 3/2 → 5/2		37 518.112 37 512.849	0.0	0.0	—	—
	6 514.3	3/2 → 3/2 3/2 → 5/2 	3/2 → 3/2 −3/2 → −3/2 3/2 → 3/2 −3/2 → −3/2	37 519.628 37 517.213 37 514.146 37 510.740	−2.910	−2.923	—	—
	9 792.2	3/2 → 3/2 3/2 → 5/2 	3/2 → 3/2 −3/2 → −3/2 3/2 → 3/2 −3/2 → −3/2	37 520.728 37 516.981 37 514.539 37 509.527	−4.380	−4.395	—	—
$0_{00} \to 1_{01}$	0.0	3/2 → 5/2 3/2 → 3/2		10 444.236 10 424.225	0.0	0.0	0	0
	13 024.7	3/2 → 5/2 3/2 → 3/2 	3/2 → 3/2 −3/2 → −3/2 3/2 → 3/2 −3/2 → −3/2	10 448.029 10 441.232 10 426.199 10 421.535	−5.730	−5.709	37	34
	19 124.7	3/2 → 5/2 3/2 → 3/2 	3/2 → 3/2 −3/2 → −3/2 3/2 → 3/2 −3/2 → −3/2	10 450.005 10 440.144 10 426.934 10 414.986	−8.405	−8.384	74	71
	24 082.3	3/2 → 5/2 3/2 → 3/2 	3/2 → 3/2 −3/2 → −3/2 3/2 → 3/2 −3/2 → −3/2	10 451.693 10 439.400 10 427.464 10 418.607	−10.575	−10.556	122	113
$1_{01} \to 1_{10}$	0.0	5/2 → 5/2		27 557.022	0.0	0.0	0	0
	22 641.1	5/2 → 5/2	5/2 → 5/2 −5/2 → −5/2	27 557.350 27 557.106	−0.244	−0.262	412	394
	24 067.0	5/2 → 5/2	5/2 → 5/2 −5/2 → −5/2	27 557.399 27 557.094	−0.305	−0.279	449	445
	25 556.6	5/2 → 5/2	5/2 → 5/2 −5/2 → −5/2	27 557.427 27 557.117	−0.310	−0.296	500	502
$1_{11} \to 2_{12}$	0.0	5/2 → 7/2 5/2 → 5/2		20 395.417 20 380.670	0.0	0.0	0	0
	16 227.3	5/2 → 7/2 5/2 → 5/2 	5/2 → 5/2 −5/2 → −5/2 5/2 → 5/2 −5/2 → −5/2	20 399.245 20 393.192 20 383.820 20 375.830	−7.022	−7.019	−43	−38
	19 086.4	5/2 → 7/2 5/2 → 5/2 	5/2 → 5/2 −5/2 → −5/2 5/2 → 5/2 −5/2 → −5/2	20 400.080 20 392.943 20 384.219 20 374.838	−8.259	−8.255	−46	−52
	24 070.9	5/2 → 7/2 5/2 → 5/2 	5/2 → 5/2 −5/2 → −5/2 5/2 → 5/2 −5/2 → −5/2	20 401.628 20 392.571 20 384.800 20 373.006	−10.425	−10.411	−84	−84
(⊥-field)								
$0_{00} \to 1_{11}$	0.0	3/2 → 5/2		37 512.849	0.0	0.0	—	—
	7 183.4	3/2 → 5/2	3/2 → 5/2 −3/2 → −5/2	37 513.073 37 512.628	−0.445	−0.449	—	—
	10 982.4	3/2 → 5/2	3/2 → 5/2 −3/2 → −5/2	37 513.194 37 512.512	−0.682	−0.686	—	—
	21 676.6	3/2 → 5/2	3/2 → 5/2 −3/2 → −5/2	37 513.519 37 512.176	−1.343	−1.355	—	—
	24 001.5	3/2 → 5/2	3/2 → 5/2 −3/2 → −5/2	37 513.611 37 512.100	−1.511	−1.500	—	—

$J_{K_-K_+} \to J'_{K'_-K'_+}$	H (Gauss)	$F \to F'$	$M_F \to M_{F'}$	ν_{obs} (MHz)	D_ν^- (MHz) obs.	D_ν^- (MHz) calc. *	D_ν^+ (kHz) obs.	D_ν^+ (kHz) calc. *
$0_{00} \to 1_{01}$	0.0	3/2 → 5/2		10 444.236	0.0	0.0	0	0
	10 987.8	3/2 → 5/2	3/2 → 5/2 −3/2 → −5/2	10 444.446 10 444.000	−0.446	−0.458	−26	−46
	21 661.8	3/2 → 5/2	3/2 → 5/2 −3/2 → −5/2	10 444.604 10 443.701	−0.903	−0.901	−167	−181
	24 001.5	3/2 → 5/2	3/2 → 5/2 −3/2 → −5/2	10 444.635 10 443.633	−1.002	−0.999	−204	−223
$0_{00} \to 1_{01}$	0.0	3/2 → 5/2 3/2 → 3/2		10 444.236 10 424.225	0.0	0.0	–	–
	10 987.8	3/2 → 5/2 3/2 → 3/2	−1/2 → −3/2 1/2 → 3/2 −1/2 → −3/2 1/2 → 3/2	10 446.259 10 442.825 10 426.601 10 421.315	4.360	4.359	–	–
$1_{10} \to 2_{11}$	0.0	5/2 → 7/2		21 375.019	0.0	0.0	0	0
	14 291.5	5/2 → 7/2	5/2 → 7/2 −5/2 → −7/2	21 375.200 21 374.758	−0.442	−0.451	−80	−81
	23 969.5	5/2 → 7/2	5/2 → 7/2 −5/2 → −7/2	21 375.273 21 374.535	−0.738	−0.757	−230	−225
$1_{11} \to 2_{12}$	0.0	5/2 → 7/2		20 395.417	0.0	0.0	0	0
	14 291.5	5/2 → 7/2	5/2 → 7/2 −5/2 → −7/2	20 395.661 20 395.065	−0.596	−0.584	−108	−112
	20 384.0	5/2 → 7/2	5/2 → 7/2 −5/2 → −7/2	20 395.726 20 394.881	−0.845	−0.833	−227	−229

* Calculated using the Zeeman parameters given in Table 9.

Table 8. Values * of $\Delta_i(g_I, g_{aa}, g_{bb}, g_{cc}, \sigma_\alpha, \sigma_\beta)$ and $S_i(\alpha, \beta)$.

i	$CH_3O^{35}Cl$ $\Delta_{i\,obs}$	δ **	$CD_3O^{35}Cl$ $\Delta_{i\,obs}$	δ **
1	−0.5949 ± 0.0025	0.0015	−0.5867 ± 0.0006	0.0020
2	−0.5795 ± 0.0010	−0.0005	−0.5762 ± 0.0005	−0.0012
3	−0.0226 ± 0.0006	0.0004	−0.0162 ± 0.0006	−0.0010
4	−0.5617 ± 0.0009	0.0000	–	–
5	−0.5686 ± 0.0006	−0.0006	−0.5680 ± 0.0007	−0.0006
6	−0.0981 ± 0.0015	−0.0007	−0.0822 ± 0.0006	−0.0002
7	−0.0622 ± 0.0008	0.0005	−0.0547 ± 0.0005	−0.0001
8	0.5167 ± 0.0015	0.0004	0.5206 ± 0.0007	0.0002
9	–	–	−0.0405 ± 0.0007	0.0009
10	−0.0597 ± 0.0007	−0.0007	−0.0544 ± 0.0007	−0.0536

***	$(S_i \times \text{const})_{obs}$	δ **	$(S_i \times \text{const})_{obs}$	δ **
$S_2 \times 30$	21.6 ± 4.2	−3.1	25.1 ± 2.0	1.9
$S_3 \times 15$	51.6 ± 4.1	4.0	46.0 ± 2.0	0.1
$S_5 \times 210$	−145.2 ± 29.0	−5.3	−118.5 ± 14.4	−2.0
$S_7 \times 15$	−25.8 ± 2.5	−1.1	−21.5 ± 4.0	1.7
$S_9 \times 105$	–	–	−168.0 ± 7.3	−4.1
$S_{10} \times 105$	−226.0 ± 20.0	15.6	−229.0 ± 7.2	1.5

* These values were obtained putting the values listed in Table 7 a and 7 b into the relations
$D_\nu^- = 0.76227_2 \times 10^{-3} \times \Delta_i \times H_Z$
and $D_\nu^+ = S_i \times H_Z^2 / 3.99027$.

** Differences between the observed and calculated values.

*** Units are in 10^{-6} erg/G²·mole.

Table 9. Molecular g-factors, magnetic susceptibility anisotropies and nuclear shielding anisotropies.

	$CH_3O^{35}Cl$	$CD_3O^{35}Cl$
$g_I(1-\sigma)$	0.5477 ± 0.0005	0.5477 ± 0.0007
g_{aa}	−0.0598 ± 0.0006	−0.0486 ± 0.0008
g_{bb}	0.0251 ± 0.0008	−0.0212 ± 0.0008
g_{cc}	−0.0376 ± 0.0005	−0.0334 ± 0.0006
$2\chi_{aa} - \chi_{bb} - \chi_{cc}$ *	−24.7 ± 1.1	−23.2 ± 1.1
$2\chi_{bb} - \chi_{cc} - \chi_{aa}$ *	1.8 ± 2.4	0.5 ± 2.0
Molecular g-factors taking account of the nuclear shielding anisotropies.		
$g_I(1-\sigma)$	0.5478 ± 0.0005	0.5480 ± 0.0009
g_{aa}	−0,0593 ± 0.0008	−0.0478 ± 0.0010
g_{bb}	−0.0249 ± 0.0009	−0.0215 ± 0.0010
g_{cc}	−0.0379 ± 0.0006	−0.033 ± 0.0009
$2\sigma_{aa} - \sigma_{bb} - \sigma_{cc}$ **	5.4 ± 5.1	8.2 ± 6.4
$2\sigma_{bb} - \sigma_{cc} - \sigma_{aa}$ **	−4.5 ± 4.9	−8.3 ± 9.1

* Units are 10^{-6} erg/G²·mole. ** Units are 10^{-3}.

were described using the notation of the two limiting cases, that is (F, M_F) and (M_J, M_I).

The selection rule for weak fields is

$$\Delta F = 0, \pm 1 \qquad \begin{array}{ll} \Delta M_F = 0 & \text{(parallel field)}, \\ \Delta M_F = \pm 1 & \text{(perpendicular field)}, \end{array}$$

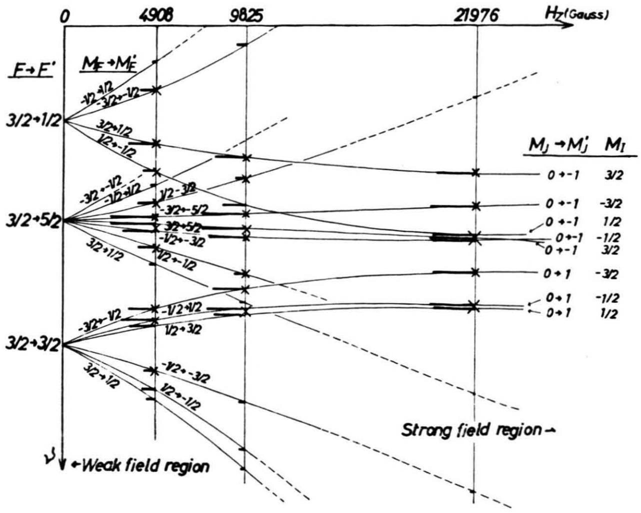

Fig. 4. Zeeman splittings of the $J=0_{00}\rightarrow J=1_{11}$ transition at perpendicular fields in CH_3OCl.

and for strong field

$$\Delta M_J=0\,,\qquad \Delta M_I=0\qquad \text{(parallel field)}\,,$$
$$\Delta M_J=\pm 1\,,\qquad \Delta M_I=0\qquad \text{(perpendicular field)}\,.$$

The Zeeman splittings of both cases in the $0_{00}\rightarrow 1_{11}$ transitions are schematically shown in Fig. 3 and in Figure 4.

The observed frequency splittings in the $CH_3O^{35}Cl$ spectrum with respect to the unperturbed lines are listed in Table 10 with the notation $(F\,M_F\,;\,M_J\,M_I)\rightarrow(F'\,M_F'\,;\,M_J'\,M_I')$ corresponding to the $(F, M_F)\rightarrow(F', M_F')$ transition at weak field limit and to the $(M_J, M_I)\rightarrow(M_J', M_I')$ transition at strong field limit.

As expected, the observed frequency splittings of the $0_{00}\rightarrow 1_{11}$ transition agree with the values calculated ignoring the second order effect of the quadrupole coupling interaction.

For the Zeeman satellites of the $1_{10}\rightarrow 2_{11}$ transition it was necessary to make the second order perturbation correction. Since the energy splittings due to the Zeeman effect is much smaller compared to the energy difference between the 2_{11} and 3_{03} levels and since the wave functions of each of the Zeeman levels at the magnetic field of 24 kG could be approximately described by the wave function $|J\,\tau\,I\,M_I\,M_J\rangle$ within an error of 10%, the second order perturbation contribution to the 2_{11} levels was calculated using the quadrupole Hamiltonian $\mathcal{H}_Q$ in the uncoupled basis as follows:

$$E^{(2)}_{2_{11}}(F\,M_F;\,M_J\,M_I)=\sum_{M_J'\,M_I'}\frac{|\langle 2_{11}\,I=3/2\,M_J\,M_I\,|\,\mathcal{H}_Q\,|\,3_{03}\,I=3/2\,M_J'\,M_I'\rangle|^2}{E_{2_{11}}-E_{3_{03}}}\,. \tag{7}$$

The matrix element of H_Q for $J'=J+1$ are obtained using the theory given by Racah [10] and are described as follows

$$\begin{aligned}\langle J\,\tau\,I\,M_J\,M_I\,|\,\mathcal{H}_Q\,|(J+1)\,\tau'\,I\,M_J'\,M_I'\rangle = C\,[&\{3\,M_I^2-I(I+1)\}\,M_J\,\sqrt{(J+M_J+1)\,(J-M_J+1)}\;\delta_{M_J' M_J}\,\delta_{M_I' M_I}\\ &\pm\tfrac{1}{2}(\pm 2\,M_I+1)\,(\pm J+2\,M_J)\,\sqrt{(I\pm M_I+1)\,(I\mp M_I)\,(J\mp M_J+2)\,(J\mp M_J+1)}\;\delta_{M_J' M_J\mp 1}\,\delta_{M_I' M_I\pm 1}\\ &\pm\tfrac{1}{2}\sqrt{(I\pm M_I+2)\,(I\pm M_I+1)\,(I\mp M_I)\,(I\mp M_I-1)\,(J\mp M_J+3)\,(J\mp M_J+2)\,(J\mp M_J+1)\,(J\pm M_J)}\\ &\cdot\delta_{M_J' M_I\mp 2}\,\delta_{M_I' M_I\pm 2}\,]\end{aligned} \tag{8}$$

where

$$C=\tfrac{1}{4}\,\chi^{\rm Cl}_{ab}\,\frac{\langle J\,\tau\,M_J=J\,|\,\Phi_{Za}\,\Phi_{Zb}+\Phi_{Zb}\,\Phi_{Za}\,|\,(J+1)\,\tau'\,M_J=J\rangle}{I(2\,I-1)\,J\,\sqrt{(2\,J+1)}}\,. \tag{9}$$

Using the Zeeman parameters of Table 9 and the nuclear quadrupole coupling constants of Table 4, the Zeeman pattern including hfs was calculated with respect to the unperturbed line and was compared to the observed one, as given in Table 10 and 11 a, b. The agreement is quite good for all the listed transitions. We take this as a final check of our Zeeman parameters and hfs constants.

In the Zeeman pattern of the $1_{11}\rightarrow 2_{12}$ and $1_{10}\rightarrow 2_{11}$ transitions measured at parallel fields, we could observe forbidden transitions which appear only at intermediate field conditions. The wave function of the Zeeman sublevel, that we call $(F\,M_F\,;\,M_J\,M_I)$, of the rotational level $J\,\tau$ is described in the basis of the functions $|J\,\tau\,I\,M_J\,M_I\rangle$ as

$$|J\,\tau\,I;\,F\,M_F;\,M_J\,M_I\rangle=\sum_{M_J'\,M_I'}C\,(J\,\tau\,I,M_J'\,M_I')\,|J\,\tau\,I\,M_J'\,M_I'\rangle \tag{10}$$

where F and M_F are quantum numbers given for the weak field case and M_J and M_I are those for the strong field case. The expansion coefficients

Table 10. Zeeman splittings $\delta\nu$ with respect to the unperturbed lines at parallel and perpendicular fields in $CH_3O^{35}Cl$. $\delta\nu^{(1)}_{obs}$'s have been calculated using rotational constants, quadrupole coupling constants and Zeeman parameters listed on Tables 4 and 9 of this paper. First order contribution only, due to the quadrupole effect, has been considered for the Zeeman splittings.

$J_{K_-K_+} \rightarrow J'_{K'_-K'_+}$	H (Gauss)	$(F\ M_F\ ;\ M_J\ M_I) \rightarrow (F'\ M_{F'};\ M_{J'}\ M_{I'})$ *	$\delta\nu_{obs}$ (MHz)	$\delta\nu^{(1)}_{calc}$ (MHz)
(‖-field)				
$0_{00} \rightarrow 1_{11}$	6 508.8	(3/2, 3/2; 0, 3/2) → (3/2, 3/2; 1, 1/2) w	6.612 ± 0.020	6.601
	19 107.9	(3/2, −3/2; 0, −3/2) → (3/2, −3/2; 0, −3/2)	3.454	3.416
	19 107.9	(3/2, 3/2; 0, 3/2) → (5/2, 3/2; 0, 3/2)	1.426	1.398
	19 107.9	(3/2, 1/2; 0, 1/2) → (5/2, 1/2; 0, 1/2)	−1.567	−1.586
	19 107.9	(3/2, −1/2; 0, −1/2) → (5/2, −1/2; 0, −1/2)	−3.170	−3.183
	6 508.8	(3/2, −3/2; 0, −3/2) → (5/2, −3/2; −1, −1/2) w	−3.298	−3.334
	6 508.8	(3/2, −1/2; 0, −1/2) → (1/2, −1/2; −1, 1/2) w	−5.806	−5.853
	6 508.8	(3/2, 1/2; 0, 1/2) → (1/2, 1/2; −1, 3/2) w	−7.716	−7.709
$0_{00} \rightarrow 1_{01}$	24 079.5	(3/2, −1/2; 0, −1/2) → (1/2, −1/2; 1, −3/2) w	26.070 ± 0.005	26.090
	24 079.5	(3/2, 1/2; 0, 1/2) → (1/2, 1/2; 1, −1/2) w	19.515	19.520
	24 079.5	(3/2, 3/2; 0, 3/2) → (5/2, 3/2; 1, 1/2) w	11.683	11.669
	24 079.5	(3/2, 1/2; 0, 1/2) → (5/2, 1/2; 0, 1/2)	7.841	7.826
	24 079.5	(3/2, −1/2; 0, −1/2) → (5/2, −1/2; 0, −1/2)	3.872	3.870
	24 079.5	(3/2, −3/2; 0, −3/2) → (5/2, −3/2; 0, −3/2)	−0.704	−0.706
	24 079.5	(3/2, 3/2; 0, 3/2) → (3/2, 3/2; 0, 3/2)	−13.586	−13.589
	24 079.5	(3/2, −3/2; 0, −3/2) → (3/2, −3/2; −1, −1/2) w	−22.486	−22.471
$1_{01} \rightarrow 1_{10}$	19 114.0	(5/2, −1/2; 0, −1/2) → (3/2, −1/2; 1, −3/2) w	10.112 ± 0.010	10.063
	13 014.2	(5/2, 1/2; 0, 1/2) → (3/2, 1/2; 1, −1/2) w	8.117	8.126
	13 014.2	(5/2, 3/2; 1, 1/2) → (3/2, 3/2; 1, 1/2)	6.728	6.720
	13 014.2	(3/2, −1/2; −1, 1/2) → (1/2, −1/2; −1, 1/2)	5.074	5.040
	24 075.8	(3/2, 1/2; −1, 3/2) → (1/2, 1/2; −1, 3/2)	−1.485	−1.501
	24 075.8	(5/2, 5/2; 1, 3/2) → (5/2, 5/2; 1, 3/2)	−6.722	−6.743
	24 075.8	(5/2, −5/2; −1, −3/2) → (5/2, −5/2; −1, −3/2)	−7.118	−7.151
	24 075.8	(5/2, 3/2; 1, 1/2) → (5/2, 3/2; 0, 3/2) w	} −10.185	{ −10.196
	24 075.8	(5/2, −3/2; 0, −3/2) → (5/2, −3/2; −1, −1/2) w		−10.214
	24 075.8	(1/2, 1/2; 1, −1/2) → (3/2, 1/2; 1, −1/2)	−1.982	−2.007
	24 075.8	(1/2, −1/2; 1, −3/2) → (3/2, −1/2; 1, −3/2)	−11.002	−11.038
$1_{11} \rightarrow 2_{12}$	22 625.5	(5/2, 3/2; 0, 3/2) → (5/2, 3/2; 0, 3/2)	−7.727 ± 0.005	−7.735
	24 083.5	(3/2, −3/2; 0, −3/2) → (7/2, −3/2; 0, −3/2) s	−4.637	−4.640
	24 083.5	(5/2, 5/2; 1, 3/2) → (5/2, 5/2; 1, 3/2)	−5.167	−5.171
	22 625.5	(1/2, 1/2; −1, 3/2) → (5/2, 1/2; −1, 3/2) s	−1.583	−1.606
	22 625.5	(3/2, 1/2; 1, −1/2) → (7/2, 1/2; 1, −1/2) s	−1.235	−1.234
	19 118.3	(3/2, −1/2; 1, −3/2) → (1/2, −1/2; 1, −3/2)	2.667	2.687
	22 625.5	(3/2, 3/2; 1, 1/2) → (3/2, 3/2; 1, 1/2)	0.096	0.099
	22 625.5	(5/2, −3/2; −1, −1/2) → (3/2, −3/2; −1, −1/2)	0.645	0.644
	24 083.5	(5/2, −5/2; −1, −3/2) → (7/2, −5/2; −1, −3/2)	2.674	2.664
	19 118.3	(1/2, −1/2; −1, 1/2) → (3/2, −1/2; −1, 1/2)	3.581	3.566
	22 625.5	(5/2, 1/2; 0, 1/2) → (3/2, 1/2; 0, 1/2)	4.919	4.909
	19 118.3	(5/2, −1/2; 0, −1/2) → (7/2, −1/2; 0, −1/2)	7.330	7.307
	22 625.5	(5/2, 1/2; 0, 1/2) → (5/2, 1/2; −1, 3/2) w	−13.146	−13.137
	22 625.5	(3/2, −3/2; 0, −3/2) → (3/2, −3/2; −1, −1/2) w	−12.471	−12.454
	22 625.5	(1/2, −1/2; −1, 1/2) → (5/2, −1/2; −2, 3/2) f	−11.971	−11.970
	22 625.5	(5/2, −1/2; 0, 1/2) → (3/2, −1/2; −1, 1/2) w	−3.470	−3.466
	19 118.3	(3/2, −1/2; 1, −3/2) → (7/2, −1/2; 0, −1/2) f	−5.273	−5.262
(⊥-field)				
$0_{00} \rightarrow 1_{11}$	4 907.6	(3/2, −1/2; 0, −1/2) → (3/2, −3/2; 0, −3/2) w	6.395 ± 0.020	6.400
	9 824.5	(3/2, −3/2; 0, −3/2) → (3/2, −1/2; 1, −3/2)	2.215	2.216
	9 824.5	(3/2, 1/2; 0, 1/2) → (5/2, −1/2; 0, −1/2) w	1.330	1.362
	9 824.5	(3/2, 1/2; 0, 1/2) → (5/2, 3/2; 0, 3/2) w	−3.470	−3.462
	4 907.6	(3/2, 1/2; 0, 1/2) → (1/2, −1/2; −1, 1/2)	−3.840	−3.819
	9 824.5	(3/2, 3/2; 0, 3/2) → (1/2, 1/2; −1, 3/2)	−4.534	−4.550
$0_{00} \rightarrow 1_{01}$	14 702.1	(3/2, 3/2; 0, 3/2) → (1/2, 1/2; 1, −1/2) w	25.762 ± 0.005	25.766
	14 702.1	(3/2, 3/2; 0, −3/2) → (1/2, −1/2; 1, −3/2)	17.694	17.704
	14 702.1	(3/2, −1/2; 0, −1/2) → (1/2, 1/2; 1, −1/2)	13.473	13.490
	14 702.1	(3/2, 1/2; 0, 1/2) → (5/2, −1/2; 0, −1/2) w	9.795	9.783
	14 702.1	(3/2, −1/2; 0, −1/2) → (5/2, −3/2; 0, −3/2) w	7.004	6.995
	14 702.1	(3/2, 3/2; 0, 3/2) → (5/2, 5/2; 1, 3/2)	4.538	4.530
	14 702.1	(3/2, −3/2; 0, −3/2) → (5/2, −5/2; −1, −3/2)	3.841	3.827

$J_{K_{-}U_{+}} \rightarrow J'_{K'_{-}K'_{+}}$	H (Gauss)	$(F\ M_F\ ;\ M_J\ M_I) \rightarrow (F'\ M_{F'}\ ;\ M_{J'}\ M_{I'})$ *	$\delta\nu_{\text{obs}}$ (MHz)	$\delta\nu^{(1)}_{\text{calc}}$ (MHz)
	14 702.1	(3/2, 1/2; 0, 1/2) → (5/2, 3/2; 1, 1/2)	2.420	2.412
	14 702.1	(3/2, −1/2; 0, −1/2) → (5/2, 1/2; 0, 1/2) w	0.051	0.046
	14 702.1	(3/2, −3/2; 0, −3/2) → (5/2, −1/2; 0, −1/2) w	−2.486	−2.493
	14 702.1	(3/2, 3/2; 0, 3/2) → (3/2, 1/2; −1, 3/2)	−11.228	−11.228
	14 702.1	(3/2, 1/2; 0, 1/2) → (3/2, −1/2; −1, 1/2)	−12.895	−12.903
	14 702.1	(3/2, −1/2; 0, −1/2) → (3/2, −3/2; −1, −1/2)	−13.833	−13.831
	14 702.1	(3/2, 1/2; 0, 1/2) → (3/2, 3/2; 0, 3/2) w	−20.824	−20.823
	14 702.1	(3/2, −1/2; 0, −1/2) → (3/2, 1/2; −1, 3/2) w	−23.507	−23.504
	14 702.1	(3/2, −3/2; 0, −3/2) → (3/2, −1/2; −1, 1/2) w	−25.188	−25.180
$1_{11} \rightarrow 2_{12}$	21 955.2	(5/2, 3/2; 0, 3/2) → (5/2, 1/2; −1/2, 3/2)	−6.955 ± 0.025	−6.963
	21 955.2	(1/2, −1/2; −1, 1/2) → (5/2, −3/2; −2, 1/2) s	−6.691	−6.694
	21 955.2	(3/2, 1/2; 1, −1/2) → (7/2, 3/2; 2, −1/2) s	−4.147	−4.151
	21 955.2	(3/2, 3/2; 1, 1/2) → (7/2, 5/2; 2, 1/2) s	−1.651	−1.660
	21 955.2	(3/2, 3/2; 1, 1/2) → (3/2, 1/2; 0, 1/2)	0.101	0.085
	21 955.2	(3/2, −3/2; 0, −3/2) → (1/2, −1/2; 1, −3/2)		0.101
	21 955.2	(1/2, 1/2; −1, 3/2) → (5/2, −1/2; −2, 3/2) s	0.581	0.552
	21 955.2	(5/2, −5/2; −1, −3/2) → (7/2, −3/2; 0, −3/2)	0.917	0.919
	21 955.2	(3/2, 1/2; 1, −1/2) → (7/2, −1/2; 0, −1/2) s	1.301	1.330
	21 955.2	(5/2, −1/2; 0, −1/2) → (3/2, −3/2; −1, −1/2)	3.461	3.453
	21 955.2	(1/2, −1/2; −1, 1/2) → (3/2, 1/2; 0, 1/2)	3.821	3.827
	21 955.2	(5/2, 1/2; 0, 1/2) → (3/2, 3/2; 1, 1/2)		4.825
	21 955.2	(5/2, −5/2; −1, −3/2) → (7/2, −7/2; −2, −3/2)	4.877	4.853
	21 955.2	(5/2, −1/2; 0, −1/2) → (7/2, 1/2; 1, −1/2)		4.874
	21 955.2	(5/2, 5/2; 1, 3/2) → (7/2, 7/2; 2, 3/2)	5.861	5.848
	21 955.2	(3/2, −1/2; 1, −3/2) → (1/2, 1/2; 2, −3/2)	9.121	9.155
	21 955.2	(3/2, −3/2; 0, −3/2) → (5/2, −5/2; −2, −1/2) w	−21.595	−21.589
	21 955.2	(3/2, −3/2; 0, −3/2) → (3/2, −1/2; −1, 1/2) w	−18.859	−18.843
	21 955.2	(3/2, 3/2; 1, 1/2) → (5/2, 5/2; 1, 3/2) w	−18.115	−18.100
	21 955.2	(1/2, 1/2; −1, 3/2) → (3/2, −1/2; −1, 1/2) w	15.797	15.778
	21 955.2	(1/2, 1/2; −1, 3/2) → (1/2, −1/2; 1, −3/2) w	34.733	34.723

w Allowed only in the weak field case.
s Allowed only in the strong field case.
f Forbidden in both cases.
* Converges to $F\ M_F \rightarrow F'\ M_{F'}$ at weak field and to $M_J\ M_I \rightarrow M_{J'}\ M_{I'}$ at strong field.

$C(J\tau, M_J'\ M_I')$ are obtained by solving the secular equation at given magnetic field H_Z.

The summation is taken over all possible values of M_J' and M_I' which give the same value of $M_F = M_J' + M_I'$.

The dipole moment matrix element corresponding to a transition from a Zeeman sublevel $|J\tau I; F\ M_F; M_J\ M_I\rangle$ to a Zeeman sublevel $|J^*\tau^* I, F^*\ M_F^*, M_J^*\ M_I^*\rangle$ is given as

$$\begin{aligned}\langle J\tau I;\ F\ M_F;\ M_J\ M_I \,|\, \mu_g\, \Phi_{Fg} \,|\, J^*\tau^* I;\\ F^*\ M_F^*;\ M_J^*\ M_I^*\rangle = \sum_{M_J' M_I' M_J'' M_I''} C\,(J\tau I, M_J'\ M_I') \quad (11)\\ \cdot C\,(J^*\tau^* I, M_J''\ M_I'')\\ \cdot \langle J\tau I\, M_J'\ M_I' \,|\, \mu_g\, \Phi_{Fg} \,|\, J^*\tau^* I\, M_J''\ M_I''\rangle\end{aligned}$$

where μ_g is the dipole moment along the g-principal axis and Φ_{Fg} is the directional cosine operator between the space fixed axis F and the principal axis g.

As the non-vanishing matrix elements in the sum (11) are given for parallel fields by the relation

$$M_J' = M_J'' \quad \text{and} \quad M_I' = M_I''$$

the selection rule for transitions between the Zeeman sublevels in the intermediate field case can be derived considering only the M_J and M_I values consistent with $M_J + M_I = M_F$.

M_F is the quantum number of the weak field limiting case but is used here as an index since both F and M_F are no more good quantum numbers. Transitions are allowed when the two sublevels have the same value of M_F and the restriction given from ΔF is taken out, that is, usual selection rules $\Delta F = 0, \pm 1$ are not applicable here. For perpendicular fields the non-vanishing matrix elements are given by the relation $M_J' = M_J'' + 1$ and $M_I' = M_I''$.

The selection rule is $\Delta M_F = \pm 1$ independent of the "index" F. According to the first of these selection rules we observed several "weak and strong field forbidden" lines in the $1_{11} \rightarrow 2_{12}$ and $1_{10} \rightarrow 2_{11}$ transitions at parallel fields. They are

$$(F = 3/2, M_F = -1/2; M_J = 1, M_I = -3/2) \\ \rightarrow (F = 7/2, M_F = -1/2; M_J = 0, M_I = -1/2)$$

Table 11 a. Zeeman splittings of the $1_{10} \rightarrow 2_{11}$ transition with respect to the unperturbed line at strong field approximation in $CH_3O^{35}Cl$.

H (Gauss)	$M_J \rightarrow M_J'$	M_I	$\delta\nu_{obs}$ * (MHz)	$\delta\nu_{calc}$ ** (MHz)		
				$\delta\nu^{(1)}$	$\delta\nu^{(2)}$	$\delta\nu_{total}$
(‖-field)						
24 067.2	$0 \rightarrow 0$	−3/2	−10.026	−10.147	0.134	−10.013
24 067.2	$1 \rightarrow 1$	1/2	−6.235	−6.430	0.191	−6.239
24 067.2	$1 \rightarrow 1$	−1/2		−6.313	0.076	−6.237
24 067.2	$1 \rightarrow 1$	−3/2	−4.459	−4.592	0.153	−4.439
24 067.2	$0 \rightarrow 0$	3/2	−3.601	−3.691	0.134	−3.557
25 565.1	$1 \rightarrow 1$	3/2	0.984	0.872	0.115	0.987
25 565.1	$1 \rightarrow 1$	−1/2	1.085	0.897	0.191	1.088
25 565.1	$-1 \rightarrow 1$	−3/2	3.014	2.873	0.115	2.988
24 067.2	$0 \rightarrow 0$	1/2	4.809	4.663	0.134	4.797
24 067.2	$-1 \rightarrow -1$	1/2	5.089	5.017	0.076	5.093
24 067.2	$-1 \rightarrow -1$	3/2	8.457	8.299	0.153	8.452
24 067.2	$0 \rightarrow 0$	−1/2	8.634	8.545	0.134	8.679
(⊥-field)						
21 955.2	$0 \rightarrow -1$	−3/2	−9.488	−9.624	0.115	−9.509
21 955.2	$0 \rightarrow 1$	−3/2	−8.464	−8.596	0.153	−8.443
21 955.2	$1 \rightarrow 2$	−1/2	−7.839	−7.989	0.163	−7.826
21 955.2	$1 \rightarrow 2$	1/2		−7.955	0.105	−7.850
21 955.2	$1 \rightarrow 0$	1/2	−6.464	−6.621	0.134	−6.487
21 955.2	$1 \rightarrow 0$	−3/2		−6.567	0.134	−6.433
21 955.2	$1 \rightarrow 0$	−1/2	−5.589	−5.684	0.134	−5.550
21 955.2	$0 \rightarrow -1$	3/2	−3.164	−3.286	0.153	−3.133
21 955.2	$-1 \rightarrow -2$	−1/2	−2.688	−2.815	0.105	−2.710
21 955.2	$1 \rightarrow 2$	−3/2	−1.164	−1.223	0.124	−1.099
21 955.2	$1 \rightarrow 0$	3/2	0.036	−0.107	0.134	0.027
21 955.2	$-1 \rightarrow -2$	1/2	1.761	1.633	0.163	1.796
21 955.2	$-1 \rightarrow 0$	−3/2	2.436	2.317	0.134	2.451
21 955.2	$0 \rightarrow -1$	1/2	3.811	3.719	0.076	3.795
21 955.2	$-1 \rightarrow -2$	−3/2	4.411	4.271	0.143	4.414
21 955.2	$0 \rightarrow -1$	−1/2	6.661	6.477	0.191	6.668
21 955.2	$0 \rightarrow 1$	−1/2	7.461	7.401	0.076	7.477
21 955.2	$-1 \rightarrow -2$	3/2	10.086	9.972	0.124	10.096

* The accuracy of the frequency measurements was estimated to be ±0.010 MHz for the parallel field and ±0.025 MHz for the perpendicular field.
** The second order effect has been calculated by the strong field approximation.

Table 11 b. Zeeman splittings of satellites forbidden at strong field for the $1_{10} \rightarrow 2_{11}$ transition in $CH_3O^{35}Cl$.

H (Gauss)	$(F\ M_F\ ;\ M_J\ M_I) \rightarrow (F'\ M_F'\ ;\ M_J'\ M_I')$	$\delta\nu_{obs}$ † (MHz)	$\delta\nu_{calc}$ * (MHz)		
			$\delta\nu^{(1)}$	$\delta\nu^{(2)}$	$\delta\nu_{total}$
(‖-field)					
19 106.2	(3/2, −1/2; 1, −3/2) → (3/2, −1/2; −1, 1/2)	−20.738	−20.824	0.076	−20.748
24 067.2	(3/2, 3/2; 1, 1/2) → (5/2, 3/2; 0, 3/2)	−20.202	−20.330	0.134	−20.196
19 106.2	(3/2, −3/2; 0, −3/2) → (3/2, −3/2; −1, −1/2)	−16.890	−17.090	0.191	−16.899
24 067.2	(3/2, −1/2; 1, −3/2) → (7/2, −1/2; 0, −1/2) f	−13.013	−13.127	0.134	−12.993
19 106.2	(5/2, −5/2; −1, −3/2) → (5/2, −5/2; −2, −1/2)	−8.126	−8.206	0.105	−8.101
24 067.2	(5/2, −1/2; 0, −1/2) → (3/2, −1/2; −1, 1/2)	−2.641	−2.697	0.076	−2.621
24 067.2	(5/2, −3/2; −1, −1/2) → (7/2, −3/2; 0, −3/2)	9.747	9.612	0.134	9.746
19 106.2	(5/2, 5/2; 1, 3/2) → (7/2, 5/2; 2, 1/2)	10.631	10.519	0.105	10.624
19 106.2	(5/2, 1/2; 0, 1/2) → (7/2, 1/2; 1, −1/2)	11.810	11.717	0.076	11.793

† Estimated error ±0.010 MHz.
f Forbidden transition in the weak and strong field approximation.
* The second order effect has been calculated in the uncoupled basis.

and

$$(F=1/2, M_F=-1/2; M_J=-1, M_I=1/2) \rightarrow (F=5/2, M_F=-1/2; M_J=-2, M_I=3/2)$$

marked in the Tables 10 and 11 b with the symbol f. The very good agreement between observed and calculated splittings confirms the values obtained for the Zeeman parameters.

3) Molecular Electric Quadrupole Moment and Second Moment Anisotropies

Combining the molecular g-factors, the magnetic susceptibility anisotropies and the rotational constants, the diagonal elements of the molecular electric quadrupole tensor can be calculated using the equation:

$$Q_{aa} = -\frac{\hbar\,|e|}{8\pi M_p}\left(\frac{2\,g_{aa}}{A} - \frac{g_{bb}}{B} - \frac{g_{cc}}{C}\right) - \frac{2\,m\,c^2}{|e|}\,(2\,\chi_{aa} - \chi_{bb} - \chi_{cc})\,. \quad (12)$$

Q_{bb} and Q_{cc} are obtained by cyclic permutation. In (12) $|e|$ is the electron charge, M_p the proton mass, m the electron mass and c the velocity of light. The values of Q_{gg} are listed in Table 12. Further the anisotropies of the second moment were calculated using the molecular structure [5] by:

$$\langle b^2\rangle - \langle a^2\rangle = \sum_n Z_n (b_n^2 - a_n^2) + \frac{\hbar}{4\pi M_p}\left(\frac{g_{bb}}{B} - \frac{g_{aa}}{A}\right) + \frac{4\,m\,c^2}{3\,e^2} \cdot \{(2\,\chi_{bb} - \chi_{aa} - \chi_{cc}) - (2\,\chi_{aa} - \chi_{bb} - \chi_{cc})\} \quad (13)$$

where Z_n is the atomic number of the n-th nucleus, and a_n and b_n are its coordinates in the principal axes. $\langle c^2\rangle - \langle b^2\rangle$ and $\langle a^2\rangle - \langle c^2\rangle$ are obtained by cyclic permutation. The resulting values are listed in Table 12. As expected, the values of the molecular quadrupole moment and the anisotropy of the second moment in $CH_3O^{35}Cl$ agree with those in $CD_3O^{35}Cl$.

The negative values of Q_{cc} in CH_3OCl and $HO^{35}Cl$ [1] can be understood considering that lone pair electron clouds are out of the plane of symmetry.

Table 12. Molecular quadrupole moments, nuclear second moments and second moment of electronic charge anisotropies.

	$CH_3O^{35}Cl$	$CD_3O^{35}Cl$
molecular quadrupole moments *		
Q_{aa}	4.6 ± 1.0	4.0 ± 1.0
Q_{bb}	-0.9 ± 1.9	-0.8 ± 1.7
Q_{cc}	-3.5 ± 2.9	-3.2 ± 2.7
nuclear second moments **		
$\sum_n Z_n a_n^2$	44.20	43.93
$\sum_n Z_n b_n^2$	5.72	5.67
$\sum_n Z_n c_n^2$	1.62	1.62
second moment of electronic charge anisotropies ***		
$\langle b^2\rangle - \langle a^2\rangle$	-37.7 ± 0.4	-37.6 ± 0.3
$\langle c^2\rangle - \langle b^2\rangle$	-3.7 ± 0.4	-3.7 ± 0.4
$\langle a^2\rangle - \langle c^2\rangle$	41.4 ± 0.8	41.3 ± 0.7

* Units are 10^{-26} esu·cm^2.
** Units are 10^{-16} cm^2. Values are calculated using the molecular structure given by Rigden et al. [3].
*** Units are 10^{-16} cm^2.

4) Electric Dipole Moment

The Stark effect of both isotopic species has been measured. To simplify the analysis the Stark displacements of components with maximum M_F of the Q-branch lines have been measured. For the $0_{10} \rightarrow 1_{11}$ transition in $CD_3O^{35}Cl$ the displacements have been analysed using the strong field approximation. The absorption cell was calibrated with the $J = 1 \rightarrow J' = 2$ transition of OCS, taking the dipole moment of OCS as 0.7152 D [11].

The measured displacement $\Delta\nu$ and the dipole moments obtained are listed in Table 13. The total

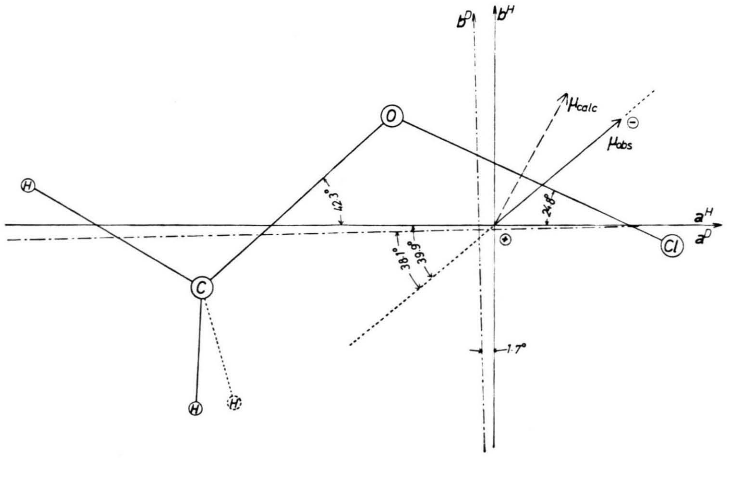

Fig. 5. Schema of the molecule $CH_3O^{35}Cl$ in the $a-b$ plane. Arrows give orientation and sign of the observed and calculated electric dipole moment. μ_{calc} was obtained by a CNDO/2 calculation.

dipole moment of $CH_3O^{35}Cl$ agrees with that of $CD_3O^{35}Cl$ within the experimental error.

As can be seen in Fig. 5 an isotopic substitution of the hydrogen atoms causes a counterlockwise rotation of the principal axes, a and b, by an angle of 1.7°.

As the total dipole moment is the same for both isotopic species different μ_a and μ_b components result in the corresponding principal axis systems. The μ_a component increases from 1.373 D to 1.409 D going from the normal to the isotopic species of the molecule. The μ_b component on the contrary decreases from 1.146 D to 1.106 D. These values are only consistent with a dipole moment having the orientation indicated by the dotted line in Figure 5.

Though the molecular g-factors of the two isotopic species have been determined, the sign of the dipole moment could not be determined experimentally. The experimental error in the obtained g-factors makes it difficult to discuss the sign of the dipole moment from this point of view.

However an information about the sign of the dipole moment was obtained by a theoretical CNDO/2 calculation [13] which gives $\mu_a = 0.78$ D and $\mu_b = 1.44$ D with direction and sign given by the broken line in Figure 5. The result is reasonable from simple chemical considerations.

Acknowledgements

We thank Mr. M. Andolfatto for the preparation of the substances. The authors express their thanks to the members of the Kiel laboratory for many helpful discussions. Further we thank the Deutsche Forschungsgemeinschaft and the Fonds der Chemie for a post-doctoral fellowship (M. S.) and for research funds. Calculations have been made with the PDP10 and X8 of the Rechenzentrum der Universität Kiel.

Appendix I

The submatrices for $J = 0$, 1 and 2 of the Hamiltonian (2) including nuclear shielding are given in Table 1 A, 2 A and 3 A. In the limit of vanishing nuclear shielding, they agree with those given in Table 1 a, 1 b and 1 c of [1].

Table 13. Stark effect and electric dipole moment.

	$J_{K_-K_+} \rightarrow J'_{K'_-K'_+}$	$(M_J\ M_I)$	Slope MHz (kV/cm)$^{-2}$ obs.	calc.
($CH_3O^{35}Cl$)				
	$1_{01} \rightarrow 1_{10}$	$(\pm 1, \pm 3/2)$	195.5 ± 1.0	–
	$4_{04} \rightarrow 4_{13}$	$(\pm 4, \pm 3/2)$	$9{,}06 \pm 0.08$	–
		$\mu_a = 1.373 \pm 0.004$ D		
		$\mu_b = 1.146 \pm 0.007$ D		
		$\mu_{total} = 1.788 \pm 0.008$ D		
($CD_3O^{35}Cl$)				
	$0_{00} \rightarrow 1_{11}$ *	$(0, \pm 3/2)$	19.55 ± 0.04	19.33
		$(0, \pm 1/2)$	19.42 ± 0.04	
	$1_{01} \rightarrow 1_{10}$	$(\pm 1, \pm 3/2)$	261.6 ± 0.5	262.1
	$4_{04} \rightarrow 4_{13}$	$(\pm 4, \pm 3/2)$	11.42 ± 0.05	11.45
	$5_{05} \rightarrow 5_{14}$	$(\pm 5, \pm 3/2)$	8.71 ± 0.06	8.90
		$\mu_a = 1.409 \pm 0.004$ D		
		$\mu_b = 1.106 \pm 0.008$ D		
		$\mu_{total} = 1.791 \pm 0.008$ D		

* The strong field approximation has been used.

1 M. Suzuki and A. Guarnieri, Z. Naturforsch. **20 a**, 497 [1975].
2 F. Scappini and A. Guarnieri, Z. Naturforsch. **31 a**, 369 [1976].
3 J. S. Rigden and S. S. Butcher, J. Chem. Phys. **40**, 2109 [1964].
4 Sandmeyer, Ber. Deutsch. Chem. Gesellschaft **19**, 859 [1886].
5 D. Sutter, Z. Naturforsch. **26 a**, 1644 [1971].
6 J. K. Bragg, Phys. Rev. **74**, 533 [1948].
7 A. M. Mirri, F. Scappini, and G. Cazzoli, J. Mol. Spectrosc. **38**, 218 [1971].
8 W. Hüttner and W. H. Flygare, J. Chem. Phys. **47**, 4137 [1967].
9 Y. Saito, Can. J. Chem. **43**, 2530 [1965].
10 G. Racah, Phys. Rev. **62**, 438 [1942].
11 J. S. Muenter, J. Chem. Phys. **48**, 4544 [1968].
12 C. H. Townes, G. C. Doumanis, R. L. White, and R. F. Schwarz, Discussions Faraday Soc. **19**, 56 [1955].
13 J. A. Pople and D. L. Beveridge. "Approximate Moleculare Orbital Theory", McGraw-Hill Book Comp., New York 1970.